Unsteady Thin Liquid Film Flow on a Porous Stretching Cylinder

Susanta Maity, Palky Handique and Swatilekha Nag

***Abstract*—Development of viscous thin liquid film is investigated over an unsteady porous horizontal non-uniformly stretching cylinder with effects of magnetic field and suction/injection. The full set of momentum equations are taken for examination under the assumption that the film thickness is uniform. Analytical and numerical solutions are obtained for the governing set of nonlinear PDEs. It is found that the film thickness diminished with increasing the cylinder radius whereas film thickness enhanced in the presence of porous medium and magnetic field. It has been observed that film thickness reduced for suction through the surface of the cylinder but reverse scenario is found for injection.**

***Index Terms*—Unsteady flow, thin film, stretching cylinder, viscous liquid, porous medium, magnetic field.**

I. Introduction

In the past decade, the development of unsteady thin incompressible viscous liquid film on a stretchable surface has gained huge applications in many industrial processes like coating of wire and fiber material, production of rubber and plastic sheets, polymer processing, etc. The steady flow of viscous fluid over a flat stretchable surface was first initiated by Crane [1] under the assumption that the sheet is moving with a linear velocity and boundary layer approximation. Subsequently, many researchers reinvestigated the problem of Crane [1] by taking different aspects of fluid mechanics. Such as, Pavlov [2] analyzed the MHD boundary layer flow on a stretchable flat sheet. Andersson et al. [3] examined the boundary layer flow on a stretching sheet with chemical reaction effect. Cortel [4] considered the effects on nonlinear motion of the sheet and heat transfer. Hayat et al. [5] studied the boundary layer flow of Jeffrey fluid on a stretching sheet. Tian et al. [6] investigated MHD stagnation-point nanofluid flow on a stretching sheet. Saif et al. [7] explored the influences of homogeneous and heterogenous chemical reactions on the flow of viscous fluid on a nonlinear stretching sheet. Recently, Reman et al. [8], Sattar et al. [9] and Farooq et al. [10] investigated the effects of Sutterby nanoliquid, Jeffery-Hamel flow and MHD flow over a nonlinear stretching sheet.

Wang [11] first investigated the boundary layer axisymmetric flow of incompressible fluid over the surface of a hollow horizontal cylinder that is stretched along the axial direction. Later, Ishak et al. [12] considered the effects of magnetic field and heat transfer over a steady stretchable cylindrical surface. Mukhopadhyay [13] studied the convective boundary layer flow over a porous stretching cylinder with temperature variation. Abbas et al. [14] probed the unsteady flow over a shrinking cylinder with slip effect. Malik et al. [15] explored the flow of magnetohydrodynamic tangent hyperbolic fluid due to stretchable cylinder. Recently, Gholinia [16], Soomro et al. [17], Waini et al. [18], Salahudin [19], Gajjela and Garvandha [20] investigated the viscous boundary layer flow on a stretching cylinder with the effects of CNTs nanofluid, shrinking cylinder, hybrid-nonofluid, Carreau fluid model, chemical reaction, etc.

The research works listed above are restricted to the boundary layer flow of infinite fluid medium. Wang [21] first studied unsteady boundary layer flow of a viscous liquid having finite film thickness that varies with time only. In this study, he restricted himself for those type of motion that obeys a specified family of time dependence and this special type of velocity field helps to select a suitable similarity transformation that ultimately transformed the boundary layer equation to a set of dimensionless ODEs, and finally solved the equations numerically. Later, several researchers, Andersson et al. [22], Dandapat et al. [23], Hayat et al. [24] Benos et al. [25], Naganthran et al. [26] have attempted the problem to study effects of heat and mass transfer, non-Newtonian liquid, thermocapillarity, MHD, slip etc. Wang [27] analyzed the boundary-layer flow of thin film on a stretching cylinder. Recently, Gul et al. [28] considered the CNTs nanoliquid film flow on a stretching cylinder. Physically, the boundary-layer that developed due to forward motion of the sheet grows fast and ultimately cover whole film thickness. Consequently, to study the flow problem, one should take the full Navier-Stokes equations instead of boundary-layer equations. Based on the above physical situation, Dandapat and Maity [29] and Dandapat et al. [30] first examined the unsteady film flow on stretching sheet by taking full set of momentum equations along with the deformable film surface.

The unsteady thin film development over a stretching cylinder by considering the full set of momentum equations has not been considered till now. In this article, the unsteady thin film development over a stretching cylinder is modeled by considering full set of Navier-Stokes equations. The effects of the porous medium, magnetic field and suction/injection are considered for analysis. It is assumed that the liquid film over the stretching cylinder is planar and it remains planar for the entire stretching time.

II. Modelling of the flow problem

A. Mathematical formulation

Considered the motion of thin liquid film on a porous stretching cylindrical surface with effects of uniform trans-

Manuscript received September 23, 2020; revised July 23, 2021. This work was supported by the Science and Engineering Research Board (SERB), New Delhi, India with the grant number EMR/2016/005174.

Susanta Maity is an assistant professor in the Department of Basic and Applied Science, National Institute of Technology, Arunachal Pradesh, Yupia, Papumpare-791112, India (e-mail:susantamaiti@gmail.com).

Palky Handique is a Ph.D. student in the Department of Basic and Applied Science, National Institute of Technology, Arunachal Pradesh, Yupia, Papumpare-791112, India (e-mail:hpalky93@gmail.com).

Swatilekha Nag is a Ph.D. student in the Department of Basic and Applied Science, National Institute of Technology, Arunachal Pradesh, Yupia, Papumpare-791112, India (e-mail:swatidkj103@gmail.com).

verse magnetic field and suction/injection (Figure 1). We denote velocity in (r, z) directions as (u, w). The film thickness $h(t)$ remains planar through out the stretching mechanism. Let the cylindrical surface at $r = a$ is stretched impulsively from the rest with velocity $C(t)z$, where a is the radius of the cylinder and $C(t)$ time depended constant. A uniform magnetic field of constant strength B_0 acts along the r direction. The equation of continuity and momentum

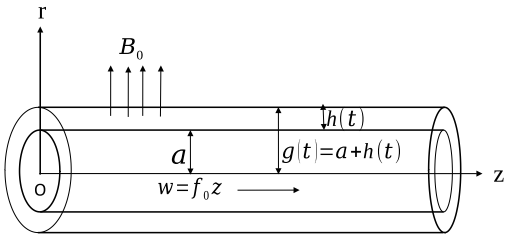

Fig. 1. Sketch of the flow geometry.

for the axisymmetric flow of incompressible fluid can then be written as:

$$\frac{1}{r}\frac{\partial(ru)}{\partial r} + \frac{\partial w}{\partial z} = 0, \tag{1}$$

$$\frac{\partial u}{\partial t} + u\frac{\partial u}{\partial r} + w\frac{\partial u}{\partial z} = -\frac{1}{\rho}\frac{\partial p}{\partial r} + \nu\left[\frac{\partial}{\partial r}(\frac{1}{r}\frac{\partial(ru)}{\partial r}) + \frac{\partial^2 u}{\partial z^2}\right] - \frac{\phi\nu u}{k}, \tag{2}$$

$$\frac{\partial w}{\partial t} + u\frac{\partial w}{\partial r} + w\frac{\partial w}{\partial z} = -\frac{1}{\rho}\frac{\partial p}{\partial z} + \nu\left[\frac{1}{r}\frac{\partial}{\partial r}(r\frac{\partial w}{\partial r}) + \frac{\partial^2 w}{\partial z^2}\right] - \frac{\phi\nu}{k}w - \frac{\sigma B_0^2}{\rho}w, \tag{3}$$

where ρ, p , ν and σ are the density, pressure, kinematic viscosity and electric conductivity of the liquid, respectively. $k(> 0)$, $\phi(0 < \phi < 1)$ are the permeability and porosity of the porous medium.

The no-slip boundary condition at $r = a$ are:

$$u = -u_s, \quad w = C(t)z, \tag{4}$$

where u_s is taken to be positive or negative according to suction or injection at cylindrical surface.

The free surface boundary conditions at $r = g(t)(= a+h(t))$ are the zero tangential stress, the balance between the normal stress and the ambient pressure and kinematic condition respectively,

$$\mu\left(\frac{\partial w}{\partial r} + \frac{\partial u}{\partial z}\right) = 0, \tag{5}$$

$$p_a - p + 2\mu\frac{\partial u}{\partial r} = 0, \tag{6}$$

$$\frac{dg}{dt} = u, \tag{7}$$

where p_a is the atmospheric pressure.

The initial conditions (at $t = 0$) are

$$u = 0, \quad w = 0, h = h_0. \tag{8}$$

B. Similarity transformation

The following similarity transformations are introduced (see Dandapat [31], Usha and Ravindran [32]),

$$\left.\begin{aligned} u(r, z, t) = u(r, t), w(r, z, t) = zf(r, t), \\ p(r, z, t) = -\frac{z^2}{2}A(r, t) + B(r, t), \end{aligned}\right\} \tag{9}$$

in the governing equations (1)-(3). Set of equations (10)-(13) are obtained after comparing the coefficient of like powers of r from both sides as,

$$\frac{1}{r}\frac{\partial(ru)}{\partial r} + f = 0, \tag{10}$$

$$\frac{\partial f}{\partial t} + u\frac{\partial f}{\partial r} + f^2 = -\frac{A}{\rho} + \nu\left[\frac{1}{r}\frac{\partial(rf)}{\partial r}\right] - (\frac{\phi\nu}{k} + \frac{\sigma B_0^2}{\rho})f, \tag{11}$$

$$\frac{\partial u}{\partial t} + u\frac{\partial u}{\partial r} = -\frac{1}{\rho}\frac{\partial B}{\partial r} + \nu\left[\frac{\partial}{\partial r}(\frac{u}{r})\right] - \frac{\phi\nu}{k}u, \tag{12}$$

$$\frac{\partial A}{\partial r} = 0. \tag{13}$$

The reduced boundary and initial conditions are:

at $r = a$

$$u(r, t) = -u_s, f(r, t) = C(t), \tag{14}$$

at the surface $r = g(t) = a + h(t)$

$$A = 0, B = 2\mu\frac{\partial u}{\partial r}, \qquad \frac{\partial f}{\partial r} = 0, \tag{15}$$

$$\frac{dg}{dt} = u, \tag{16}$$

at $t = 0$

$$f = 0, u = 0, h = h_0. \tag{17}$$

We obtained $A(r, t) = 0$ by solving the equations (13) with the help of (15). The value of $B(r, t)$ may be found from equation (12) after integration with respect to r.

C. Scaling

The non-dimensional form of the above system of equations are obtained by the following dimensionless variables

$$R = \frac{r}{h_0}, \tau = tC_0, F = \frac{f}{C_0}, U = \frac{u}{u_0}, H = \frac{h}{h_0}, A = \frac{a}{h_0}, G = \frac{g}{h_0}, \tag{18}$$

where $u_0(= h_0C_0)$, C_0 are the characteristic velocity, and initial stretching strength respectively.

The dimensionless set of equations are

$$\frac{1}{R}\frac{\partial(RU)}{\partial R} + F = 0, \tag{19}$$

$$Re\left[\frac{\partial F}{\partial \tau} + U\frac{\partial F}{\partial R} + F^2\right] = \frac{1}{R}\frac{\partial}{\partial R}(R\frac{\partial F}{\partial R}) - (Mn^2 + \beta)F, \tag{20}$$

where, $Re = \frac{h_0^2 f_0}{\nu}$, $Mn = B_0 h_0 \sqrt{\frac{\sigma}{\mu}}$, $\beta = \frac{\phi h_0^2}{k}$ are the Reynolds number, the Hartmann number and the porosity parameter respectively.
The dimensionless boundary and initial conditions are given below.
At $R = A$:

$$U = -V, \quad F = \frac{C(\tau)}{C_0}, \tag{21}$$

where $V = u_s/u_0$ is the non-dimensional suction/injection velocity and $V > 0$ or $V < 0$ according to suction and injection, respectively.
At film surface $R = G(\tau) = A + H(\tau)$:

$$\frac{\partial F}{\partial R} = 0, \tag{22}$$

$$\frac{dG}{d\tau} = U. \tag{23}$$

At time $\tau = 0$:

$$F = U = 0, H = 1. \tag{24}$$

III. Asymptotic solution for small Re

The analytical solutions of the nonlinear governing equations (19)-(20) are derived by perturbation methods. We assume that $C(\tau) = C_0$, $Re << 1$. We also assume that Hartman number Mn^2 and porosity parameter β are of order Re. We expanded dependent variables in the power of Re as

$$\Phi(R, \tau) = \sum \epsilon^j \Phi_j(R, \tau). \tag{25}$$

We found a set of PDE's by comparing the coefficients of like power of Re from both sides after substitution of the equation (25) into the equations (19)-(20). Finally, solving these equations and we found the velocity components F, U as,

$$F = 1 + Re(1 + \overline{Mn}^2 + \overline{\beta})[\frac{1}{4}(R^2 - A^2)^2 - \frac{G^2}{2}\ln(R/A)], \tag{26}$$

$$U = \frac{(A^2 - R^2 - 2VA)}{2R} + Re(1 + \overline{Mn}^2 + \overline{\beta})\left[\frac{(A^4 - R^4)}{16R} + \frac{1}{8R}(A^2 - R^2)(G^2 - A^2) + \frac{G^2}{4}R\ln(R/A)\right]. \tag{27}$$

In the aforementioned $Mn^2 = Re\overline{Mn}^2$, $\beta = Re\overline{\beta}$ and $\overline{Mn}^2$, $\overline{\beta}$ are of $O(1)$. The film evolution equation (28) is derived by substituting (27) into the kinematic condition (23) as

$$G\frac{dG}{d\tau} = \frac{1}{2}(A^2 - G^2) - VA + Re(1 + \overline{Mn}^2 + \overline{\beta})\left[-\frac{(G^4 - A^4)}{16} + \frac{1}{8}(A^2 - G^2)(G^2 - A^2) + \frac{G^4}{4}\ln(G/A)\right]. \tag{28}$$

Following the above asymptotic expansion (25) in equation (28), we found the equation (29) for film thickness at $O(Re^0)$ as

$$G_0\frac{dG_0}{d\tau} = \frac{1}{2}(A^2 - G_0^2) - VA, \tag{29}$$

whereas at $O(Re^1)$ we get,

$$\frac{d(G_0G_1)}{d\tau} + G_0G_1 = (1 + \overline{Mn}^2 + \overline{\beta})\left[\frac{1}{16}(A^4 - G_0^4) - \frac{1}{8}(A^2 - G_0^2)^2 + \frac{G_0^4}{4}\ln(G_0/A)\right]. \tag{30}$$

Solving equations (29) and (32), we obtained the analytical expression of film thickness as

$$H(\tau) = -A + \sqrt{A^2 + c_0e^{-\tau} - 2VA} + \frac{Re}{\sqrt{A^2 - 2VA + c_0e^{-\tau}}} \times \left[c_1e^{-\tau} + (1 + \overline{Mn}^2 + \overline{\beta})\left[-\frac{c_0^3e^{-3\tau}}{48A^2} + \frac{c_0^3V}{8A^3}e^{-3\tau} + \left(\frac{V^2A^2}{4} - \frac{c_0VA}{4} + \frac{3}{2}c_0V^2 - V^3A\right)\tau e^{-\tau} + \left(\frac{c_0^2V^2}{4A^2} + \frac{c_0V}{2A}\right)e^{-2\tau}\right]\right], \tag{31}$$

where c_0 and c_1 are the integration constants which we determined here by the initial condition as $c_0 = 1 + 2(A + V)$ and $c_1 = -(1 + \overline{Mn}^2 + \overline{\beta})\left[-\frac{c_0^3}{48A^2} + \frac{c_0^3V}{8A^3} + \frac{c_0^2V^2}{4A^2} + \frac{c_0V}{2A}\right]$.

IV. Numerical solution

The numerical solution of the problem is obtained with the higher values of Re, Mn and β by using the finite difference technique. The traditional finite difference technique can't be used here as the boundary for film thickness always varies with time. The physical region $[0, H(\tau)]$ is therefore transformed to a fixed domain $[0, 1]$ for numerical computation. The transformation (32) (see, [33]) is considered to translate the moving physical domain into a fixed numerical-computational domain.

$$\eta(\tau) = 1 - a_1 \ln\left(\frac{a_2H(\tau) - (R - A)}{b_2H(\tau) + (R - A)}\right), \quad 1 < c < \infty, \tag{32}$$

where $a_1 = [\ln(a_2/b_2)]^{-1}$, $a_2 = c + 1$ and $b_2 = c - 1$, c is the grid spacing parameter in physical domain.
Equation (20) is discretized by the Crank-Nicholson finite difference technique. The nonlinear term F^2 is estimated by the Newton's linearization technique (Fletcher [34]). The numerical iterations are carried out with the following tridiagonal system of linear algebraic equations,

$$PF_{j-1}^{n+1} + QF_j^{n+1} + RF_{j+1}^{n+1} = (S)_j^n, \tag{33}$$

where,

$$P = \frac{B - A}{4\delta\eta} - \frac{C}{2\delta\eta^2},$$

$$Q = \frac{1}{\delta\tau} + \frac{C}{\delta\eta^2} + 2F_j^n,$$

$$R = \frac{A - B}{4\delta\eta} - \frac{C}{2\delta\eta^2},$$

$$(S)_j^n = F_j^n\left[\frac{1}{\delta\tau} + F_j^n - \frac{C}{\delta\eta^2} - \frac{Mn^2}{Re} - \frac{\beta}{Re}\right] + F_{j-1}^n\left[\frac{A - B}{4\delta\eta} + \frac{C}{2\delta\eta^2}\right] + F_{j+1}^n\left[\frac{B - A}{4\delta\eta} + \frac{C}{2\delta\eta^2}\right],$$

$$A = \frac{a_1(a_2 + b_2)(H^nW_j^n - (R(j) - A)\frac{dH}{d\tau})}{(a_2H^n - (R(j) - A))(b_2H^n + (R(j) - A))},$$

$$B = \frac{a_1(a_2 + b_2)H}{R(j)Re(a_2H^n - (R(j) - A))(b_2H^n + (R(j) - A))}$$

$$+\frac{a_1(a_2+b_2)H^n[(b_2-a_2)H^n+2(R(j)-A)]}{Re(a_2H^n-(R(j)-A))^2(b_2H^n+(R(j)-A))^2},$$

$$C=\frac{1}{Re}\left[\frac{a_1(a_2+b_2)H^n}{(a_2H^n-(R(j)-A))(b_2H^n+(R(j)-A))}\right]^2.$$

At a fixed time level F is computed from the above tridiagonal system equations (33). Hence, U and H are computed from the equation of continuity and kinematic condition respectively.

The computation of the variables F, U and H will continue until satisfying the following convergence criterion:

$$\frac{\sum_j |K_j^{n+1}-K_j^n|}{\sum_j |K_j^{n+1}|}\leq \epsilon, \tag{34}$$

where $K=(F,U,H)$, ϵ is the convergence criterium which is taken as $\epsilon=10^{-6}$.

The numerical simulation is done with 51 grid points along

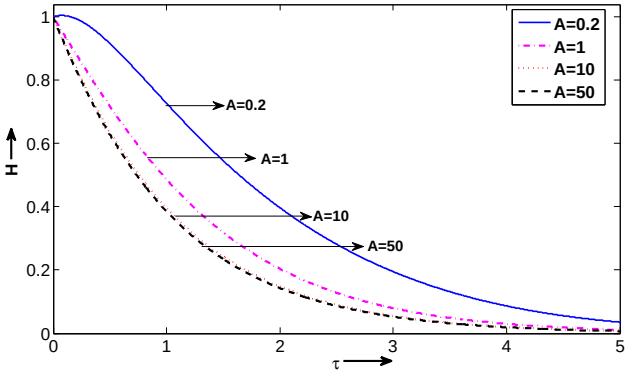

Fig. 2. Variation of H with time τ for different values of A when $Re=0.1$, $Mn=1$, $\beta=1$, $V=-0.01$.

with $c=10^4$ and this gives the uniform grid distribution in computational domain. The time step for numerical computation is taken as

$$\delta\tau\leq 0.25\times\delta\eta^2, \tag{35}$$

which comes from the Courant-Friedrichs-Lewy (CFL) condition of numerical stability.

V. Results and Discussion

In figure 2, we have plotted analytical expression (31) for film thickness H with time τ for various values of non-dimensional radius A of the cylinder. It is found that the film thickness diminishes with increasing values of A but it can be seen that the results for $A=10$ and above are indistinguishable. Figure 3 shows the numerical simulation of film height H for several values of Hartmann number Mn. It is seen that film thinning rate decreases with increasing values of Mn. This happens as the Lorentz force resists the motion of the liquid film and it produces more resistance for higher values of Mn. Figure 4 has illustrated the computation of H with time τ for different porosity parameter β and observed that film height enhances as β increases. The porosity of the porous medium ϕ on the surface of the stretching cylinder raises for higher β and resists the motion of the liquid film. The influence of suction/injection velocity V on film thinning process is depicted in figure 5. As shown in figure 5(a), the film thinning rate increased with the higher

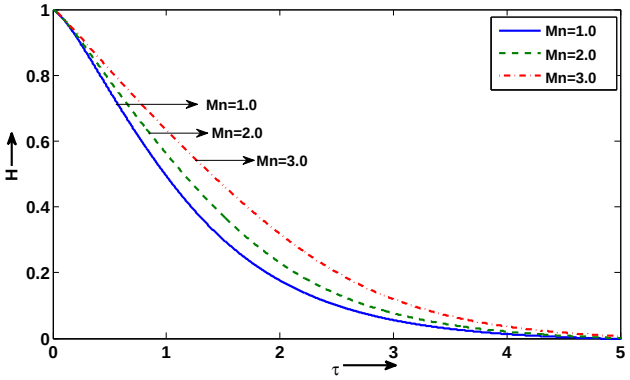

Fig. 3. Variation of H with time τ for different values Hartmann number Mn when $Re=1.0$, $\beta=1$, $A=2$, $V=0.01$.

suction velocity at the surface of the cylinder. In figure 5(b), the opposite scenario is noticed for injection. Figure 6 (a) and 6 (b) reveals the change of velocities F and U across the film height at various time steps τ. From figure 6 (a), it is seen that F increases gradually to achieve its stretching velocity for large τ. Due to impulsive stretching, the velocity of the cylinder first imparted to the adjacent liquid layer, and then it spread out the entire film thickness by the viscous action. Further, it is found that F is maximum at the surface of the cylinder, and it diminished as film thickness increases. It is also found from the graph that film height declined with time. From figure 6 (b), it is observed that the vertical velocity U diminished with raising time. Figure 7 (a) and 7 (b) depicts the impacts of Hartmann number Mn and porosity parameter β on the radial velocity F. From figure 7 (a), it is observed that velocity F reduces insignificantly with higher values of Mn. It is to be mentioned here that in the

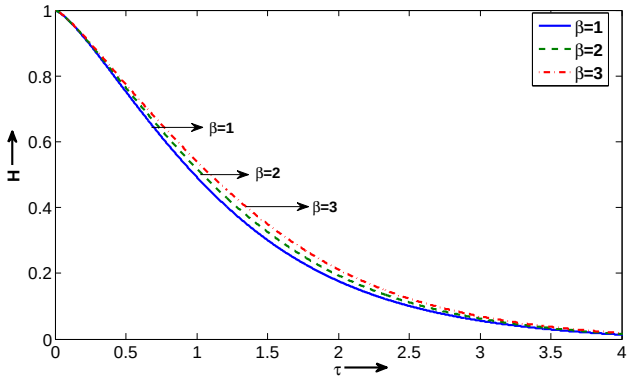

Fig. 4. Variation of H with time τ for different values of porosity parameter β when $Re=1.0$, $Mn=1$, $A=2$, $V=0.01$.

presence of magnetic field a retarding body force known as the Lorentz force is generated along the transverse direction of the applied magnetic field. This Lorentz force opposes the liquid motion and F reduces with raising Mn. It is also obvious that the velocity component F decreases with β. The porosity of the porous medium exerts resisting force to the liquid motion as it restricts the flow of liquid along the surface of the cylinder. The porosity parameter β heightens due to the higher of porosity of the porous medium. As a result, the velocity F decreases with β. Figure 8 portrays the velocity component F with R for different values of V at a fixed time. The velocity F increases with the higher values

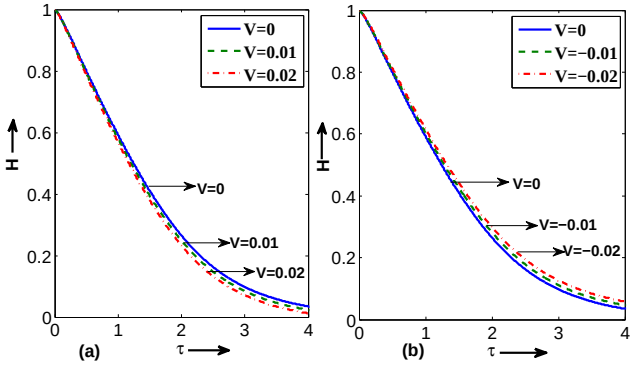

Fig. 5. Variation of H with τ for different values of suction/injection velocity V when $Re = 1.0$, $Mn = 2$, $\beta = 2$, $A = 2$.

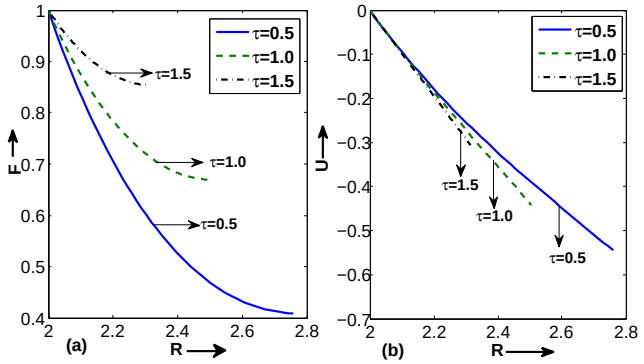

Fig. 6. Variation of velocity compontes with respect to R for different time when $Re = 1.0$, $Mn = 1$, $\beta = 1$, $A = 2$ and $V = -0.01$. Here, (a) for F and (b) for U.

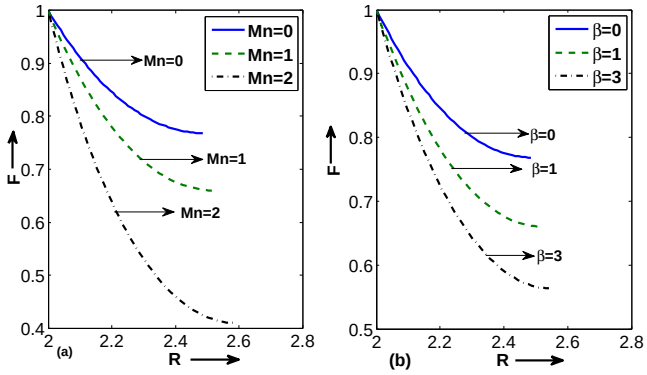

Fig. 7. Variation of F with R when $Re = 1.0$, $A = 2$ and $V = -0.01$ and $\tau = 1$. Here, (a) for different Mn with $\beta = 1$ and (b) for different β with $Mn = 1$.

of suction velocity at the cylindrical surface but reverse phenomenon is observed for injection. For suction from the surface of cylinder there will be continuous loss of the liquid mass from the system. As a result, the remaining liquid moves faster along the stretching direction. For the injection through the surface of the cylinder, the system continuously gains more liquid mass resulting in slow motion. Now, the impact of different stretching possibilities of the cylinder and their consequence viz. when the cylinder

(i) is stretched impulsively from rest and maintains its constant velocity C_0 for further time as $C(\tau) = C_0$,

(ii) is stretched impulsively from rest and increases its velocity continuously with time τ as $C(\tau) = C_0(1 - \delta\tau)^{-1}$, where $(\delta\tau) < 1$ and

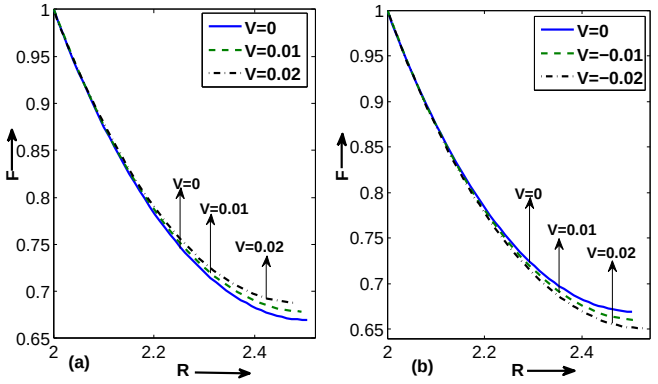

Fig. 8. Variation of F with R for different suction/injection velocity when $Re = 1.0$, $Mn = 1$, $\beta = 1$, $A = 2$ and $\tau = 1$. Here, (a) for suction and (b) for injection.

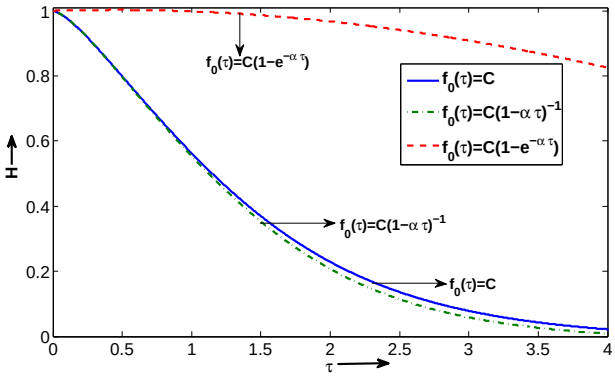

Fig. 9. Variation of film thickness H for different stretching speed when $Re = 1.0$, $Mn = 1$, $\beta = 1$, $A = 2$ and $V = -0.01$.

(iii) is stretched from rest and increases its velocity with time to attain a constant finite value $C(\tau) = C_0(1 - e^{-\delta\tau})$ as $\tau \to \infty$ is presented in figure 9. It is observed from the figure that the change of film height for three cases of stretching is markedly different. The film thinning rate is more for the stretching of type (ii). One may expect that the film thickness for the cases (i) and (iii) coincides after a substantial time.

VI. Conclusion

Flow and development of thin viscous liquid film on an unsteady stretching cylindrical surface are analyzed with influence of transverse magnetic field and porous medium. In the mathematical model the full set of Navier-Stokes equations are included under the assumption that the film thickness is uniform throughout the time. Both the analytical and numerical solutions are obtained for nonlinear governing set of PDEs. The major conclusions from the above analysis are as follows:

1) Thickness of viscous liquid film H reduces for increasing values of radius of the cylinder A. But this result is indistinguishable for large values of A.
2) Thickness of viscous liquid film H enhances for increasing values of the Hartmann number Mn and porosity parameter β.
3) Thickness of viscous liquid film H declines for suction on the cylindrical surface whereas the film thickness increases for injection.

4) The velocity of the liquid film attends maximum value at the stretching cylindrical surface and it slows down along the film thickness.
5) The rate of film thinning is more for the continuously increasing stretching speed of the cylinder compared to constant stretching.

REFERENCES

[1] L. E. Crane, "Flow past a stretching plane," *J. Appl. Maths. Phys. (ZAMP)*, vol. 21, pp. 645-647, 1970.

[2] K. B. Pavlov, "Magnetohydrodynamic flow of an incompressible viscous fluid caused by deformation of a plane surface," *Magnitnaya Gidrodinamika (U.S.S.R.)*, vol. 4, pp. 146-147, 1974.

[3] Helge I. Andersson, Olav R. Hansen and B. Holmedal, "Diffusion of a chemically reactive species from a stretching sheet," *Int. J. Heat Mass Trans.*, vol. 37, pp. 659-664, 1994.

[4] R. Cortell, "Viscous flow and heat transfer over a nonlinearly stretching sheet," *Appl. Math. Comput.*, vol. 184, no. 2, pp. 864873, 2007.

[5] T. Hayat, R.S. Saif, R. Ellahi, T. Muhammad and A. Alsaedi, "Simultaneous effects of melting heat and internal heat generation in stagnation point flow of Jeffrey fluid towards a nonlinear stretching surface with variable thickness," *Int. J. Therm. Sci.*, vol. 132, pp. 344-354, 2018.

[6] Xi-Yan Tian, Ben-Wen Li and Zhang-Mao Hu, "Convective stagnation point flow of a MHD non-Newtonian nanofluid towards a stretching plate," *Int. J. Heat Mass Trans.*, vol. 127, pp. 768-780, 2018.

[7] R. S. Saif, T. Muhammad, H. Sadia and R. Ellahid, "Boundary layer flow due to a nonlinear stretching curved surface with convective boundary condition and homogeneous-heterogeneous reactions," *Physica A: Statistical Mechanics and its Applications*, vol. 551, pp. 123996, 2020.

[8] S. Rehman, N. A.Mira, M. Farooq, M. Rizwan, F. Ahmad, S. Ahmad, and B. Ahmad, "Analysis of thermally stratified flow of Sutterby nanofluid with zero mass flux condition," *J. Mater. Res. Tech.*, vol.9, no. 2, pp. 1631-1639, 2020.

[9] A. Sattar J. A. Al-Saif and A. M. Jasim, " Analytical investigation of the MHD Jeffery-Hamel flow through convergent and divergent channel by new scheme," *Engineering Letters*, vol. 27, no. 3, pp.646-657, 2019.

[10] M. A. Farooq, R. Sharif and A. Mushtaq, "Numerical comparison of constant and variable fluid properties for MHD flow over a nonlinearly stretching sheet, " *IAENG Int. J. Appl. Math.*, vol. 50, no. 2, pp. 384-395, 2020.

[11] C. Y. Wang, "Fluid flow due to a stretching cylinder," *Phys Fluids*, vol. 31, pp.466-468, 1988.

[12] A. Ishak, R. Nazar, I. Pop, "Magnetohydrodynamic flow and heat transfer due to a stretching cylinder," *Energy Convers. Manage.*, vol. 49, pp. 3265-3269, 2008.

[13] S. Mukhopadhyay, "Mixed convection boundary layer flow along a stretching cylinder in porous medium,"*J. Petrol. Sci. Eng.*, vol. 96, pp. 73-78, 2012.

[14] Z. Abbas, S. Rasool and M. M. Rashidi, "Heat transfer analysis due to an unsteady stretching/shrinking cylinder with partial slip condition and suction," *Ain Shams Eng. J.*, vol. 6, pp. 939-945, 2015.

[15] M. Y. Malik, T. Salahuddin, H. Arif and S. Bilal, "MHD flow of tangent hyperbolic fluid over a stretching cylinder:Using Keller box method," *J. Magn. Magn. Mater.*, vol. 395, pp. 271-276, 2015.

[16] M.Gholinia, M.Armin, A. A. Ranjbar and D. D. Ganji, "Numerical thermal study on CNTs/ $C_2H_6O_2$-H_2O hybrid base nanofluid upon a porous stretching cylinder under impact of magnetic source", *Case Studies in Thermal Engineering*, vol.14, pp. 100490, 2019.

[17] F. A. Soomro, A. Zaib, R. Ul Haq and M. Sheikholeslami, " Dual nature solution of water functionalized copper nanoparticles alonga permeable shrinking cylinder: FDM approach ", *Int. J. Heat and Mass Transfer*, vol. 129, pp. 1242-1249, 2019.

[18] I. Waini, A. Ishak and I. Pop, "Hybrid nanofluid flow towards a stagnation point on a stretching/shrinking cylinder," *Scientific Reports*, vol. 10, 9296, 2020.

[19] T. Salahuddin, "Carreau fluid model towards a stretching cylinder: Using Keller box and shooting method," *Ain Shams Engineering Journal*, vol.11, pp. 495-500, 2020.

[20] N. Gajjela, M. Garvandha, " The influence of magnetized couple stress heat, and mass transfer flow in a stretching cylinder with convective boundary condition, cross-diffusion, and chemical reaction", *Thermal Science and Engineering Progress*, vol. 18, pp. 100517, 2020.

[21] C. Y. Wang, "Liquid film on an unsteady stretching surface," *Q. Appl. Math.*, vol. 48, 601-610, 1990.

[22] H. I. Andersson, J. B. Aarseth, N. Braud and B. S. Dandapat, "Flow of a power-law fluid on an unsteady stretching surface," *J. Non-Newtonian Fluid Mechs.*, vol. 62, pp. 1-8, 1996.

[23] B. S. Dandapat, B. Santra and H. I. Andersson, "Thermocapillarity in a liquid film on an unsteady stretching surface," *Int. J. Heat Mass Trans.*, vol. 46, pp. 3009-3015, 2003.

[24] T. Hayat, S. Saif and Z. Abbas, "The influence of heat transfer in an MHD second grade fluid film over an unsteady stretching sheet," *Physics Letters A*, vol.372, pp. 5037-5045, 2008.

[25] L.Th. Benos, U.S. Mahabaleshwar, P.H. Sakanaka and I.E. Sarris, "Thermal analysis of the unsteady sheet stretching subject to slip and magnetohydrodynamic effects," *Thermal Sci. Engg. Progress*, vol. 13, pp. 100367, 2019.

[26] K. Naganthran, I.Hashim, R. Nazar, " Non-uniqueness solutions for the thin Carreau film flow and heat transfer over an unsteady stretching sheet," *Int. Comm. Heat Mass Trans.*, vol. 117, pp. 10477, 2020.

[27] C. Y. Wang, " Liquid film sprayed on a stretching cylinder," *Chem. Eng. Comm.*, vol. 193, pp. 869-878, 2006.

[28] T. Gul, M. Bilal, M. Shuaib, S. Mukhtar and P. Thounthong, " Thin film flow of the waterbased carbon nanotubes hybrid nanofluid under the magnetic effects," *Heat Transfer* , vol. 49, pp. 3211-3227, 2020.

[29] B. S. Dandapat and S. Maity, "Flow of a thin liquid film on an unsteady stretching sheet," *Phys. Fluids*, vol. 18, pp. 102101, 2006.

[30] B. S. Dandapat, S. Maity and A. Kitamura, "Liquid film flow due to an unsteady stretching sheet," *Int. J. Non-Linear Mechanics*, vol. 43, pp. 880-886, 2008.

[31] B. S. Dandapat, "Unsteady flow of thin liquid film on a disk under nonuniform rotation," *Phys. Fluids*, vol. 13, pp. 1860-1868, 2001.

[32] R. Usha and R. Ravindran, "Numerical study of a film cooling on a disk," *Int. J. Non-Linear Mechanics*, vol. 36, 147-154, 2001.

[33] G. O. Robert, "Lecture Notes in Physics," *Spinger-Verlag*, 1971.

[34] C. A. J. Fletcher,"Computational Techinique For Fluid Dynamics," *Spinger-Verlag*, New York, Vol.**II**, 1988.